

Integrated Computer-Aided Working-Fluid Design and Power System Optimisation: Beyond Thermodynamic Modelling

*Oyeniya A. Oyewunmi, Martin T. White, Maria Anna Chatzopoulou, Andrew J.
Haslam, Christos N. Markides*

Clean Energy Processes (CEP) Laboratory, Department of Chemical Engineering,

Imperial College London, South Kensington Campus, London SW7 2AZ, UK.

Abstract:

Improvements in the thermal and economic performance of organic Rankine cycle (ORC) systems are required before the technology can be successfully implemented across a range of applications. The integration of computer-aided molecular design (CAMD) with a process model of the ORC facilitates the combined optimisation of the working-fluid and the power system in a single modelling framework, which should enable significant improvements in the thermodynamic performance of the system. However, to investigate the economic performance of ORC systems it is necessary to develop component sizing models. Currently, the group-contribution equations of state used within CAMD, which determine the thermodynamic properties of a working-fluid based on the functional groups from which it is composed, only derive the thermodynamic properties of the working-fluid. Therefore, these do not allow critical components such as the evaporator and condenser to be sized. This paper extends existing CAMD-ORC thermodynamic models by implementing group-contribution methods for the transport properties of hydrocarbon working-fluids into the CAMD-ORC methodology. Not only does this facilitate the sizing of the heat exchangers, but also allows estimates of system costs by using suitable cost correlations. After introducing the CAMD-ORC model, based on the SAFT- γ Mie equation of state, the group-contribution methods for determining transport properties are presented alongside suitable heat exchanger sizing models. Finally, the full CAMD-ORC model incorporating the component models is applied to a relevant case study. Initially a thermodynamic optimisation is completed to optimise the working-fluid and thermodynamic cycle, and then the component models provide meaningful insights into the effect of the working-fluid on the system components.

Keywords:

ORC; CAMD; Working fluid; Optimisation; SAFT- γ Mie; Heat exchanger modelling.

1. Introduction

Reducing fossil-fuel consumption and our impact on the environment are key drivers behind the development of renewable technologies and technologies that improve energy-efficiency. An organic Rankine cycle (ORC) system is a suitable technology for the conversion of low temperature heat into power, and commercial systems are available ranging in size from a few kW up to tens of MW [1]. However, challenges such as identifying optimal working fluids which meet all necessary environmental and safety constraints, and unfavourable economics need to be addressed.

Working-fluid selection criteria have been summarised within the literature [2,3]. In a typical working-fluid selection study a group of working fluids are identified from an existing database. This group is then screened based on pre-defined environmental, safety, operational and material compatibility constraints, before a parametric optimisation study is completed in which the ORC is optimised for each screened working fluid. The optimal solution is then identified based on performance indicators such as thermal efficiency or net power output. Several of these studies can be found within the literature, for example in [4,5].

Alternatively, computer-aided molecular design (CAMD) can be used to simultaneously optimise the working fluid and the ORC system, thus removing any subjective screening criteria. In CAMD a working fluid is defined as a combination of molecular groups (e.g., $-\text{CH}_3$, $-\text{CH}_2-$, $=\text{CH}$), which are

put together in different ways to form different molecules. In the CAMD-ORC approach, integer variables describing the working fluid, and continuous variables describing the ORC, are simultaneously optimised using a mixed-integer non-linear programming (MINLP) optimiser. Figure 1 compares an integrated CAMD-ORC model to a conventional working-fluid selection study. Previous CAMD-ORC studies have paid attention to safety and environmental characteristics [6], and have demonstrated the potential of CAMD to improve efficiency in waste heat recovery applications [7]. However, these studies used empirical equations of state and did not complete a full MINLP optimisation. A more recent study [8] used a more advanced equation of state and conducted the full MINLP optimisation. However, this study only considered the ORC thermodynamic performance.

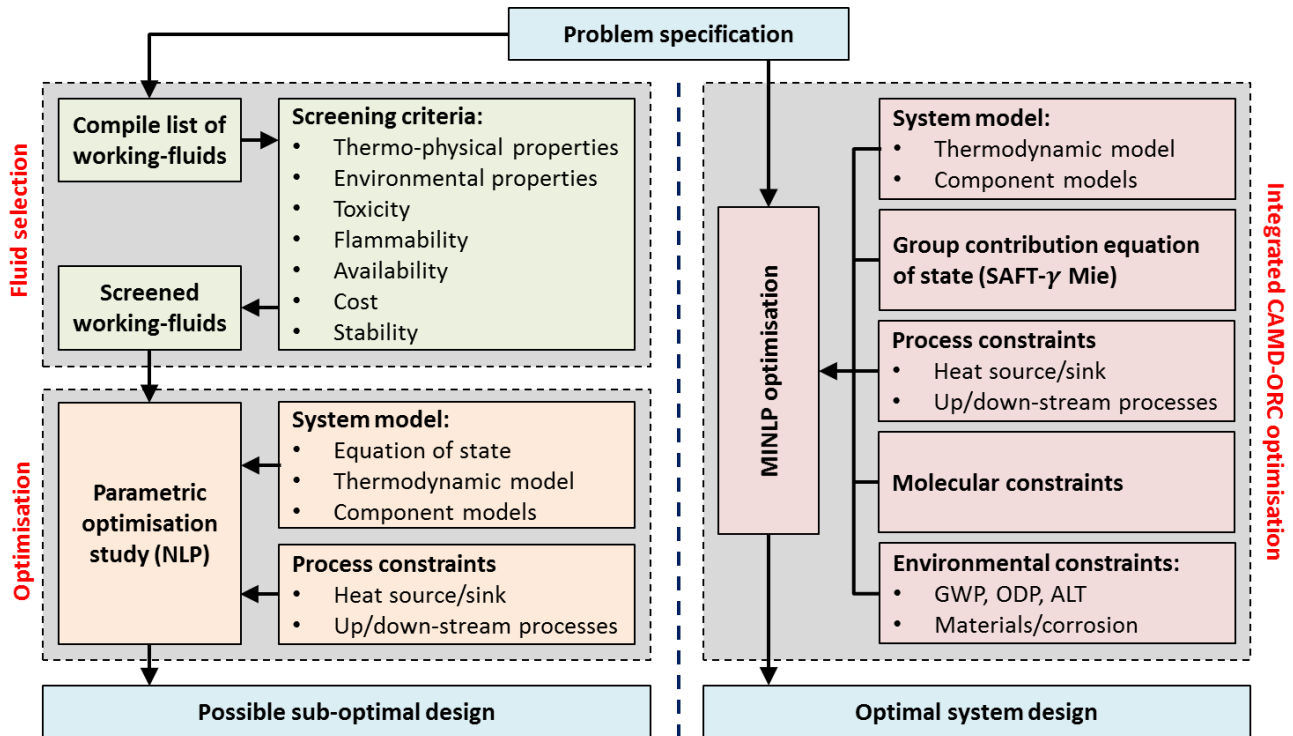


Fig. 1. Schematic of an integrated CAMD-ORC optimisation model.

The unfavourable economics of ORC systems could be enhanced through techno-economic optimisation studies. These capture the trade-off between thermodynamic performance and system cost by predicting investment costs, through suitable component sizing models and cost correlations, and then optimising a performance metric such as the specific investment cost (£/kW), payback period or net-present value. This approach has previously been used to determine optimal ORC systems for different applications [9,10]. However, the integration of these concepts within CAMD-ORC has yet to be considered. This can be partly attributed to difficulties associated with using group-contribution methods for determining transport properties, and the complexity of the optimisation process.

The aim of this paper is to move beyond existing CAMD-ORC models by introducing component sizing models into an existing CAMD-ORC framework. This consists of using group-contribution methods to predict transport properties and then implementing these methods into heat exchanger sizing models. After this introduction, the key aspects of the CAMD-ORC model, including the group-contribution methods and the heat exchanger sizing model, are summarised in Section 2, before being validated in Section 3. Finally, the model is applied to a case study in Section 4 in which the effect of the working fluid on the heat exchanger geometry is evaluated.

2. Description of the model

2.1. The CAMD-ORC model

The CAMD-ORC model has been developed in the gPROMS [11] modelling environment, and consists of a group-contribution equation of state (SAFT- γ Mie), molecular feasibility constraints, an

ORC process model and a MINLP optimiser. The CAMD-ORC model has been described previously [12], and therefore only the key aspects of this model are summarised here.

A group-contribution of state predicts the thermodynamic properties of a working fluid by considering the molecular groups that make-up the molecule. For example, propene can be described by combining three different molecular groups, namely $=CH_2$, $=CH-$ and $-CH_3$. SAFT- γ Mie is a specific type of group-contribution equation of state which is based within statistical associating fluid theory (SAFT) and uses a Mie potential to describe the interaction between two molecular groups [13]. Currently, group parameters are available for a number of molecular groups [14], including those considered within this paper ($-CH_3$, $-CH_2$, $>CH-$, $=CH_2$ and $=CH-$).

In the CAMD-ORC model, molecular constraints are required to ensure rules of stoichiometry and valence are obeyed, therefore ensuring a generated set of molecular groups represents a feasible molecule. The constraints used here are defined in [15].

The process model concerns a subcritical, non-recuperated ORC. The notation used to describe this system is given in Figure 2. The heat source and heat sink are defined by their inlet temperatures (T_{hi} , T_{ci}), mass flow rates (\dot{m}_h , \dot{m}_c) and specific heat capacities ($c_{p,h}$, $c_{p,c}$). Three variables describe the ORC; the condensation temperature T_1 , the reduced pressure $P_r = P_2/P_{cr}$, where P_{cr} is the fluid critical pressure; and the amount of superheat ΔT_{sh} . Finally, the pump and expander are both modelled by assumed isentropic efficiencies, denoted η_e and η_p , respectively.

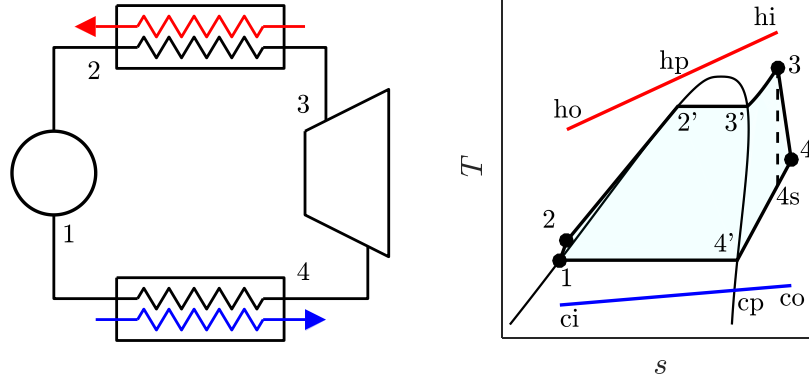


Fig. 2. Schematic of the ORC and the cycle on a T - s diagram along with the notation used in this paper.

The thermodynamic analysis of the ORC is well described within the literature, and will not be reproduced here. However, the energy balances applied to the heat addition and heat rejection processes are important to the heat exchanger sizing. Defining the evaporator pinch point ($PP_h = T_{hp} - T_{2'}$) as an additional model variable, the working-fluid mass flow rate is:

$$\dot{m}_o = \frac{\dot{m}_h c_{p,h} (T_{hi} - T_{hp})}{h_3 - h_{3'}}. \quad (1)$$

The condenser pinch point PP_c is then determined, and this must be greater than the minimum allowable pinch point $PP_{c,min}$, which is defined as a model constraint:

$$PP_c = T_{4'} - \left(T_{ci} + \frac{\dot{m}_o (h_{4'} - h_1)}{\dot{m}_c c_{p,c}} \right) \geq PP_{c,min}. \quad (2)$$

Finally, the optimisation of the process model and working fluid is carried out using the OAERAP MINLP optimiser which is built into gPROMS [11]. In the OAERAP solver the optimal solution is obtained by solving a number of non-linear programming (NLP) and mixed-integer linear programming (MILP) sub-problems, and repeating these until convergence. The objective function of the optimisation within this study is to maximise the power output the system.

In a previous study [12], the CAMD-ORC model has been successfully validated against an ORC thermodynamic coupled to REFPROP, and against a different CAMD-ORC optimisation study [8] taken from the literature.

2.2. Group-contribution transport property modelling

A key step in the sizing of heat exchangers is the estimation of the heat transfer coefficients for the different fluid phases. This process relies heavily on combinations of various thermodynamic and transport properties (which are not provided by the SAFT-based equations of state), including their thermal conductivity and dynamic viscosity. Thus, the required transport properties, specifically the dynamic viscosity, thermal conductivity and surface tension, have to be predicted by other property-estimation or group contribution methods. A number of these methods for hydrocarbon working fluids (*n*-alkanes, methyl alkanes, 1-alkenes and 2-alkenes) have been compared, contrasted and validated against experimental data from NIST/REFPROP in [16]; here, we provide a summary of those employed in this work.

2.2.1 Dynamic viscosity

The dynamic viscosities of liquid *n*-alkanes can be accurately predicted by the Joback and Reid group contribution method [17] which uses a two-parameter equation to describe the temperature dependency of the dynamic viscosity:

$$\eta_L = M \exp \left[\left(\sum_i \eta_{a,i} - 597.82 \right) / T + \sum_i \eta_{b,i} - 11.202 \right], \quad (3)$$

where η_L is the liquid viscosity in units of Pa s and M is the molecular weight of the molecule. The contributions from each group ($\eta_{a,i}$ and $\eta_{b,i}$) considered in this paper can be found in Joback and Reid [17]. This method however gives predictions with large errors for the liquid viscosities of branched alkanes. For these molecules, an alternative method, the Sastri-Rao method [18] is employed. The pure-liquid viscosity in units of mPa s is calculated with the equation:

$$\eta_L = \sum_i \eta_{B,i} \times P_{vp}^{-[0.2 + \sum_i N_i]} \quad (4)$$

The values for the group contributions to determine the summations above are given in Ref. [18] while the vapour pressure P_{vp} is calculated as a function of the normal boiling point.

For the vapour phases, the dynamic viscosities (in units of microPoise) are calculated using the corresponding states relation suggested by Reichenberg [19, 20]:

$$\eta_v = \frac{M^{1/2} T}{\sum_i n_i C_i [1 + (4/T_{cr})][1 + 0.36 T_r (T_r - 1)]^{1/6}} \times \frac{T_r (1 + 270 \mu_r^4)}{T_r + 270 \mu_r^4}, \quad (5)$$

with a correction for high pressure fluids. Here, n_i represents the number of groups of the i^{th} type and C_i is the individual group contribution and μ_r is the reduced dipole moment.

2.2.2 Thermal conductivity

Liquid thermal conductivities are calculated using the Sastri method [21]:

$$\lambda_L = \sum_i \lambda_{b,i} \times a^m, \text{ where } m = 1 - \left(\frac{1 - T_r}{1 - T_{b,r}} \right)^n \quad (6)$$

with $a = 0.856$ and $n = 1.23$ for alcohols and phenols, or $a = 0.16$ and $n = 0.2$ for other compounds, and $\lambda_{b,i}$ (in W/(m K)) is the group contribution to the thermal conductivity at the normal boiling point.

The vapour phase thermal conductivities are calculated by the Chung *et al.*, method [22, 23] as:

$$\frac{\lambda_v M'}{\eta_v c_v} = \frac{3.75 \Psi}{c_v / R} \quad (7)$$

Note that the variables in this equation are expressed in SI units, where M' is the molar mass in kg/mol, $R = 8.314$ J/(mol K), and c_v in J/(mol K) is obtainable from an equation of state such as the SAFT- γ Mie. The factor Ψ is calculated as presented in Ref. [22].

2.2.3 Liquid surface tension

Several empirical corresponding states correlations are available for the estimation of the surface tension of the various chemical families of fluids. Sastri and Rao [24] present a modification of the corresponding-states methods to deal with polar liquids:

$$\sigma = KP_{cr}^x T_b^y T_{cr}^z \left[\frac{1 - T_r}{1 - T_{b,r}} \right]^m, \quad (8)$$

where σ is the surface tension in mN/m, and the pressure and temperature terms are in units of Kelvin and bar respectively. The values of the constants for alcohols and acids are available in Ref. [24], while for all other families of compounds, $K = 0.158$, $x = 0.50$, $y = -1.5$, $z = 1.85$ and $m = 11/9$.

2.3. Heat exchanger modelling and sizing

The correct selection and sizing of the ORC system components is of key importance in order for the system performance to match the design intent. The component design is also highly related to the financial viability of the installation, because it affects significantly the ORC system investment cost.

The heat exchangers (HEXs) used for the evaporator and the condenser account for 40-70% of the ORC system cost, depending on the scale of the unit and the heat source temperature [25]. In this work, the evaporator and condenser units selected are of tube-in-tube construction. This type of HEX is cost-effective and suitable for small to medium scale capacities. To obtain credible estimates of the HEX size, the heat transfer area is needed, which in turn requires the calculation of the heat transfer coefficient (HTC). The model developed for the evaporator unit divides the component into three distinct sections: i) the preheating section, where the organic fluid is in liquid phase; ii) the evaporating section, where the organic fluid changes phase; and iii) the superheating section, where the organic fluid is in vapour phase. For each section, the HTC is calculated, using different Nusselt number correlations. The condenser unit is divided into: i) the desuperheating section, where the organic fluid is vapour; and ii) the condensing zone, where the fluid undergoes phase change.

There is a prolific amount of literature on Nusselt number correlations, obtained for different working fluids. For the single-phase zones, the most well established correlations are those of Dittus Boelter [26] and Gnielinski [27]. However, the estimation of the HTC when phase change phenomena occur is more complex, due to the continuously changing quality of the organic fluid along the length of the HEX. Further discretisation in space is required (n-segments per zone), and the HTC_i is then calculated for every segment "i". Knowing the HTC_i , and using the logarithmic mean temperature difference method (LMTD) the area requirements per segment (A_i) are obtained. By summing the areas (A_i) calculated, the overall area requirements of the HEX unit are obtained.

In this study, a number of different Nusselt number correlations for the evaporating and condensing zone have been used. For evaporation inside tubes, the correlations proposed by Cooper [28] and Gorenflo [29] have been used for nucleate boiling conditions, whereas the Dobson [30] and Zuber [28] have been used to account for the convective heat transfer phenomena. For condensation inside tubes, the correlations proposed by Shah [31] and Dobson [30] have been considered, accounting for both gravity driven and shear driven condensation.

3. Model validation and case study

3.1. Model setup and thermodynamic results

The CAMD-ORC has previously been used [12] to design the working fluid and thermodynamic cycle for three different ORC systems, designed for heat source temperatures of 150, 250 and 350 °C respectively. The results from this optimisation study will be used as the basis for the investigation completed in this paper. Alongside the three heat source temperatures, each system was also defined by the model inputs defined in Table 1.

Table 1. Model inputs for the CAMD-ORC optimisation.

$c_{p,h}$ J/(kg K)	\dot{m}_h kg/s	T_{ci} K	$c_{p,c}$ J/(kg K)	\dot{m}_c kg/s	η_p	η_e	$PP_{c,min}$ K
4200	1.0	288	4200	5.0	0.7	0.8	5

The optimisation study also considered four different hydrocarbon families, and these are summarised in Table 2. For each heat source temperature and hydrocarbon family a parametric study was completed in which the number of CH₂ groups was varied manually whilst the ORC variables (i.e., T_1 , P_r , ΔT_{sh} and PP_h) were optimised.

Table 2. Definition of the four hydrocarbon families considered within this study.

n -alkanes	methyl alkanes
$CH_3 - (CH_2)_n - CH_3$	$(CH_3)_2 - CH - (CH_2)_n - CH_3$
1-alkenes	2-alkenes
$CH_2 = CH - (CH_2)_n - CH_3$	$CH_3 - CH = CH - (CH_2)_n - CH_3$

This aim of this study was to investigate how the number of CH₂ groups affects the performance of the ORC. The results from study are summarised in Fig. 3, and are presented in terms of the number of Carbon atoms within the molecule. From a thermodynamic point of view, these results suggest n -propane, 2-pentene and 2-hexene are the optimal working fluids for the 150, 250 and 350 °C heat-source temperatures, respectively.

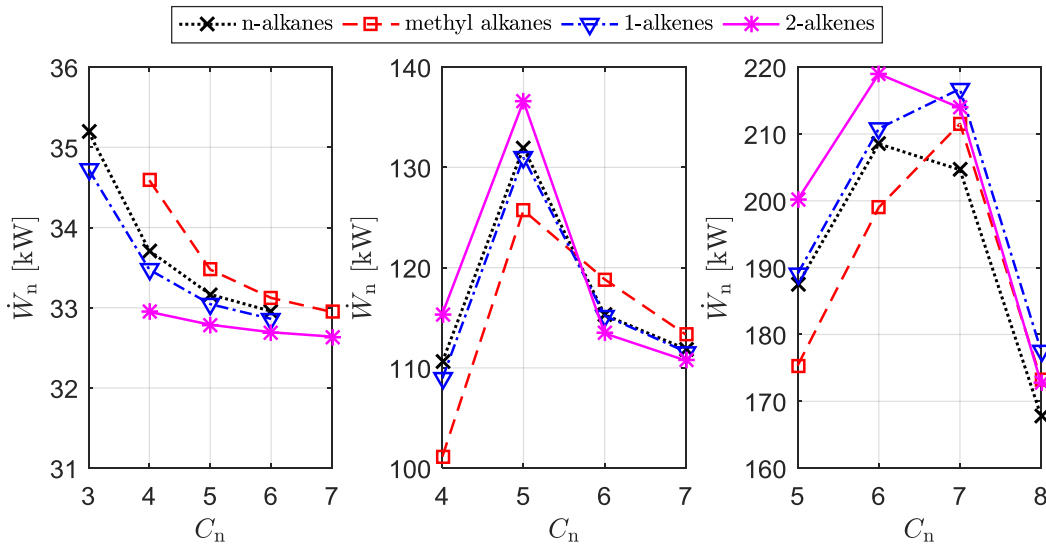


Fig. 3. The effect of the number of carbon atoms C_n contained within the working fluid on the net power output from the ORC for the four hydrocarbon families at three different heat-source temperatures; from left to right: $T_{hi} = 150, 250$ and 350 °C.

After completing this study, the number of CH₂ groups was then introduced as an optimisation variable, alongside T_1 , P_r , ΔT_{sh} and PP_h , and a MINLP optimisation was completed for the four different hydrocarbon families. The results from these studies agreed with the results shown in Fig. 3, identifying the same optimal working fluids.

The aim of the current work is to extend this work beyond thermodynamic modelling. This means assessing the effect of the number of CH₂ groups on the size of the system components, facilitating the selection of an optimal working fluid for each heat-source temperature based on non-thermodynamic performance metrics.

To size the heat exchangers, it is first necessary to redefine the heat source. Initially the heat source was defined by an arbitrary heat capacity rate (i.e., $\dot{m}_h c_{p,h}$). However, to size the heat exchanger it is necessary to fully define the heat source such that the transport properties can be predicted. For this purpose, the heat source has been redefined as a thermal oil, namely Therminol 66 [32], at 1 bar, and

the same temperature profile and heat addition within the evaporator is assumed. In this instance, the thermal oil flow rate can be determined to provide the same amount of heat to the ORC system. For the 150, 250 and 350 °C heat-source temperatures, this corresponds to a mass flow rate of 2.1 kg/s.

3.2. Validation of the component models

The HEX models introduced in Section 2.3 have been used to obtain the area requirements of the evaporator and the condenser, for the optimum cycles identified from the CAMD-ORC modelling. The HEX sizing is first performed using the NIST REFPROP [33] properties. The results are then compared to those obtained when the group contribution transport properties are used (Section 2.2). The fluids used for the comparison study include propane (*n*-alkanes), isobutane (methyl alkanes), propene (1-alkene) and cis-2-butene (2-alkene). The heat carrier fluid for all fluids is Therminol 66, entering the evaporator at 150 °C and 1 bar.

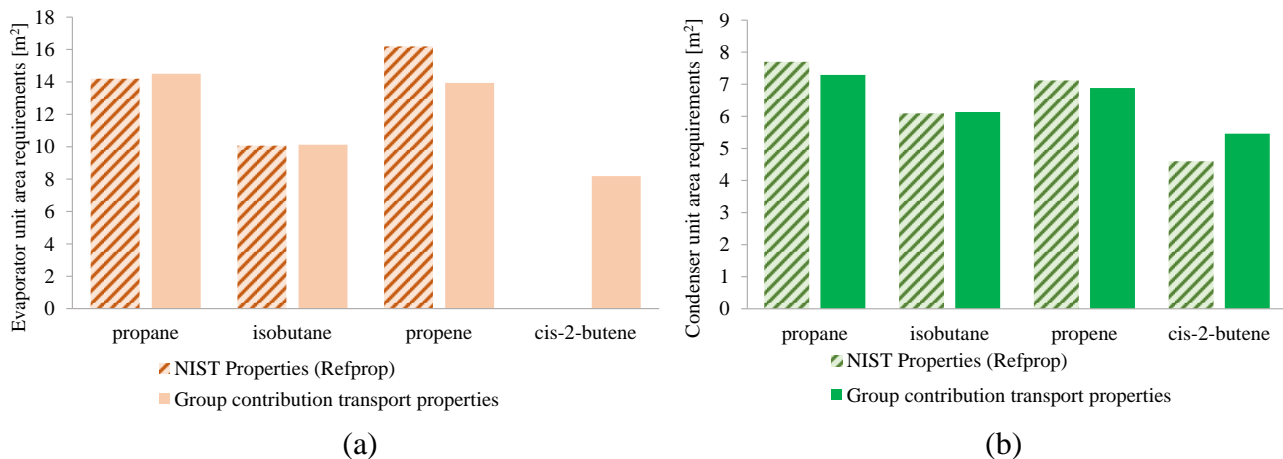


Fig. 4. HEX sizing results using NIST REFPROP and the group contribution method for: a) the evaporator and b) the condenser.

In Fig. 4a and 4b, the evaporator and condenser unit area requirements for four working fluids are presented. In line with the figures, the group contribution transport properties method results are in good agreement with those obtained from NIST REFPROP. The HEX area calculations for propane and isobutane have negligible difference between the two methods. The highest deviation is recorded for cis-2-butene, where the condenser unit surface area is overestimated by the group contribution method by approximately 18 %, being on the conservative side of the HEX design. It should be noted, that the Nusselt number correlations for the evaporator area calculation require the use of the working fluid surface tension, which for cis-2-butene is not available in NIST. Adding to this, the evaporator area requirements for propene are 16 m² when NIST properties are used, but it is approximately 14 m² when the group contribution transport properties are used (-13% deviation).

Looking at the overall HEX area variation, the highest area requirements for the evaporator are obtained for propene (from both methods), followed by propane. Both cycles generate approximately 35 kW of net power, whereas the ORC operating with isobutane and 2-butene generate approximately 33 kW and 34 kW respectively. The heat input to the ORC operating with propane and propene, is higher than the respective ones for isobutane and cis-2-butene, because the heat carrier fluid undergoes a higher temperature drop. This is attributed to the fact that the ORC with propane and propene have lower evaporating saturation temperatures, than those with isobutane and cis-2-butene, approximately 87 °C and 97 °C, respectively. This allows for a higher heat carrier fluid temperature drop, releasing more heat into the cycle. The higher heat input to the component results in larger unit size. A similar trend is observed for the condenser surface area requirements. The condenser units for propene and propane are larger than those for isobutane and cis-2-butene. However, for every working fluid, the total area requirements of the condenser are lower than the respective ones for the evaporator. This is owing to: i) the lower condenser load than the respective one in the evaporator; and ii) to the fact that most of the heat release process is done in the condensing (two-phase) zone where the HTC's achieved are higher. These factors result in lower heat transfer area requirements.

3.3. Application to the case study

After the validation of the group contribution method for calculating the transport properties, the method is used to obtain the HEX sizes for all the optimum cycles obtained from the CAMD-ORC model. In Fig. 5 the breakdown of the evaporator area into the three zones examined is presented for 12 fluids, namely the optimal *n*-alkane, methyl alkane, 1-alkene and 2-alkene working fluids for the three heat-source temperatures. This corresponds to propane, isobutane, propene and cis-2-butene for the 150 °C heat source, pentane, isopentane, 1-pentene and 2-pentene for the 250 °C heat source and hexane, isoheptane, 1-heptene and 2-hexene for the 350 °C heat source. The heat carrier fluid (Therminol 66) is fixed at 1 bar for all cases. It should be noted that fluids such as 1-pentene, 2-pentene, isoheptane, 1-heptene, and 2-hexene, are not included in the Refprop library. Therefore, without the use of the group contribution method the sizing of such systems would be impossible.

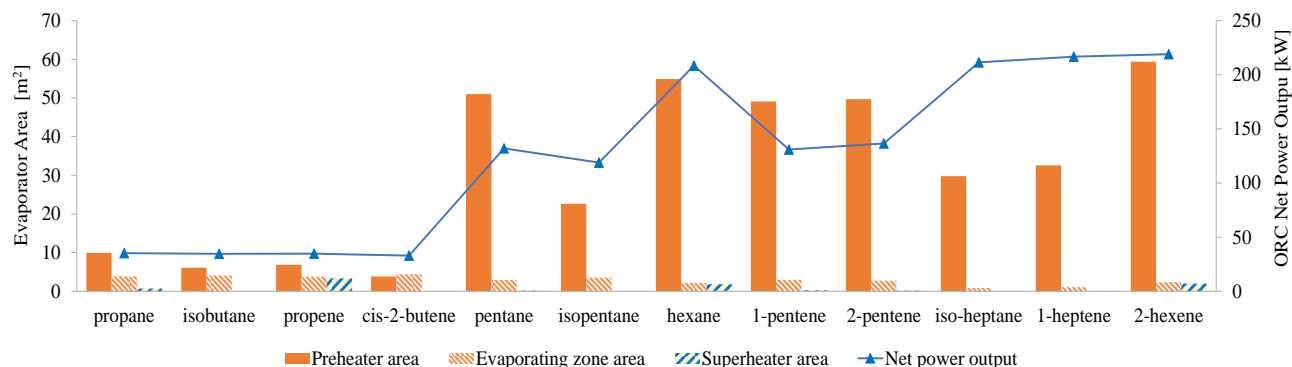


Fig. 5. Evaporator HEX area break-down using the group-contribution transport properties.

The highest heat-source temperature (350 °C) results in significantly higher power outputs, reaching 219 kW for 2-hexene, 217 kW for 1-heptene, 211 kW for isoheptane, and 209 kW for hexane (Fig. 5). These are followed by 2-pentene with 137 kW, pentane and 1-pentene with 132 kW, and isopentane with 119 kW, and correspond to the 250 °C heat source. As expected, the higher power output due to higher heat input (Fig. 6) generally results in high heat transfer area requirements for the evaporator. For the 350 °C heat sources 2-hexene has the highest area requirements reaching 64 m², followed by hexane with 54 m². Although isoheptane and 1-heptene generate almost similar power output to 2-hexene and hexane, the evaporator area requirements of the former are approximately 50% lower than the latter. The difference can be attributed to the higher temperature difference obtained across the length of the HEX with these fluids, in comparison to hexane and 2-hexene. Hexane and 1-hexene have higher evaporation temperatures than isoheptane and 1-heptene as illustrated in Fig. 6.

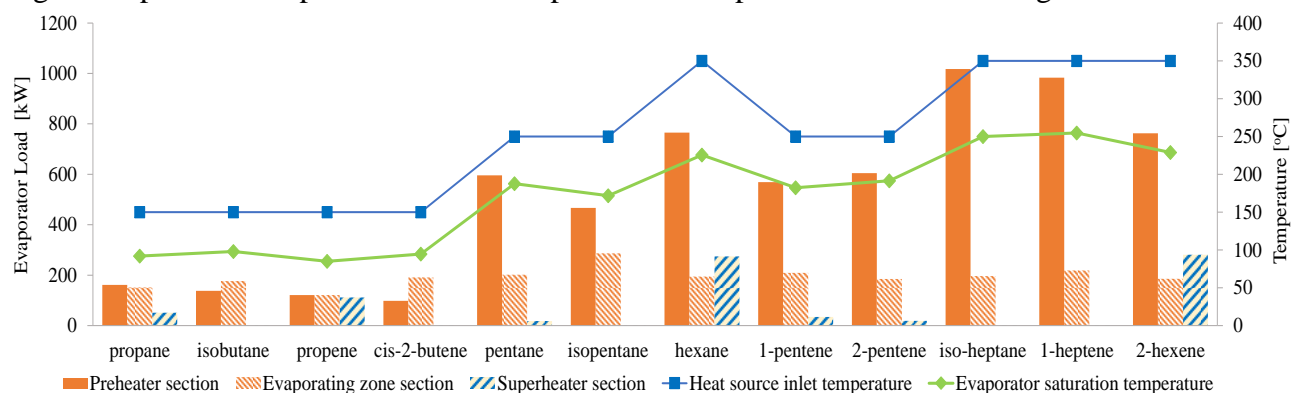


Fig. 6. Evaporator load break-down for the optimum ORC systems.

For the 250 °C heat sources, pentane, 1-pentene and 2-pentene all have similar area requirements of 53 m², and generate a similar amount of power. However, whilst there is a power reduction of 8 % when using isopentane compared to pentane, the area requirements for isopentane are 51% lower than the respective ones for pentane (Fig. 5). This difference can be attributed to several reasons; the first being that that evaporation pressure for pentane is close to the critical point, resulting in a lower latent heat load for the phase change, than for isopentane (Fig. 6). Furthermore, almost 74% of the heat transfer is

done in the preheater section, where the HTC is lower than the respective HTC achieved in the two-phase zone. Adding to this, the LMTD of the preheater section for pentane is equal to the evaporator pinch point across the full length of the HEX, resulting in high area requirements. A similar behaviour to pentane is observed for 1-pentene and 2-pentene.

In Fig. 7, the condenser HEX area break-down is illustrated. In contrast with the evaporator, for fluids such as 2-hexene, 1-heptene, isoheptane, isopentane, and hexane, the condenser area requirements do not increase significantly, although the condenser load increases (Fig. 8). This is attributed to the higher temperature differences between the heat sink, and the expander outlet temperature and the condensation temperature. In line with Fig. 8, these fluids have higher condensation temperatures (50-55 °C), compared to fluids such as propene and cis-2-butene (31-32 °C). Therefore, the LMTD is higher, resulting in lower area requirements (for the same heat load). Since, the load in the condenser for fluids such as isoheptane, 1-heptene, hexane and pentane is higher, the area increases but modestly.

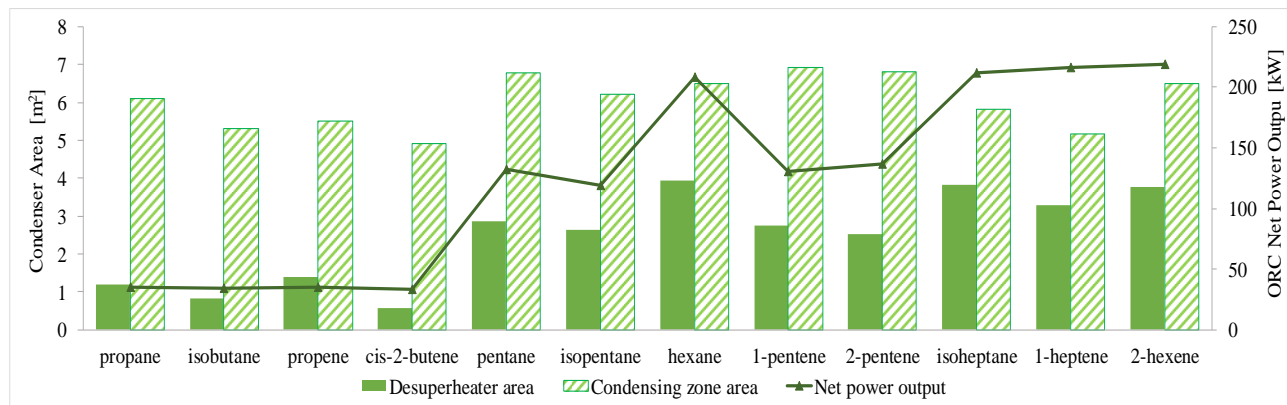


Fig. 7. Condenser HEX area break-down using the group-contribution transport properties.

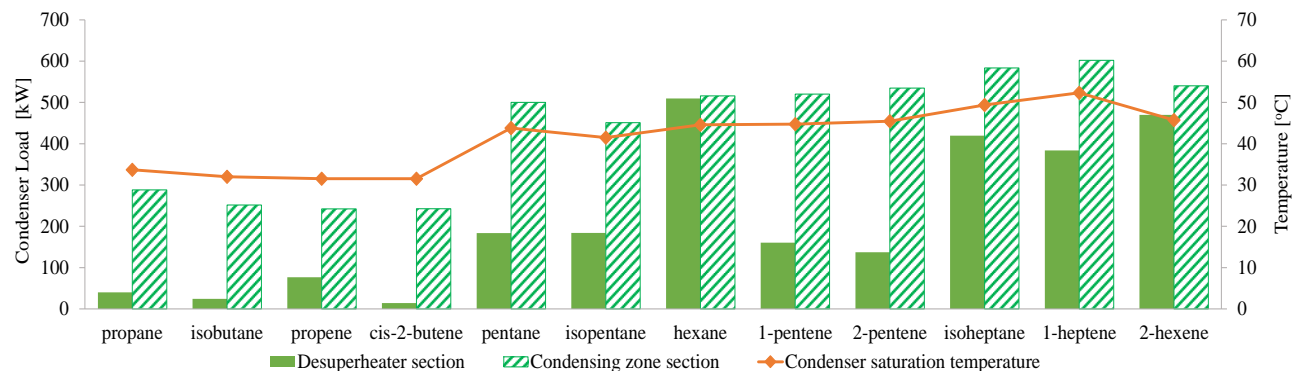


Fig. 8. Condenser load break-down for the optimum ORC systems.

4. Conclusions

The introduction of computer-aided molecular design into the optimisation of ORC systems can identify the next generation of optimal working fluids for these systems. However, existing CAMD-ORC models must be extended to include component modelling, allowing optimal systems to be identified based on techno-economic performance indicators.

This paper has integrated a discretised heat exchanger model, based on group-contribution transport properties, into an existing CAMD-ORC thermodynamic model. The model has been validated against data from NIST REFPROP, and a good agreement is found for *n*-alkane and methyl alkane working fluids. The largest deviations of +18 % and -13 % were observed when sizing the condenser for cis-2-butene, and the evaporator for propene respectively. These relatively small deviations confirm the suitability of the group-contribution transport property prediction methods. The results from a case study show that for a 350 °C heat source selecting isoheptane, or 1-heptane, over 2-hexene results in a 50 % reduction in evaporator area, with only a minimal reduction in power output. Similarly, for a 250 °C heat source, selecting isopentane instead of *n*-pentane reduces the evaporator area by 50 %, whilst corresponding to an 8 % reduction in power output. The main contributing factor to this are

higher temperature differences within the heat exchanger, owing to the differences in the optimal cycles in terms of their evaporation temperatures and amount of superheating. The required condenser areas show less variation, but in general are lower than the evaporator area requirements.

Ultimately, this study has confirmed the suitability of group-contribution methods to determine transport properties for hydrocarbon working fluids, and the results provide useful insights with respect to the effect of working fluid on the heat exchanger design. Although different working fluids may result in similar power outputs, the heat exchanger area requirements can be significantly different. This highlights the importance of integrating component models, and cost correlations, into the CAMD-ORC framework facilitating techno-economic optimisations to be completed.

Nomenclature

A	area, m^2
c_p	specific heat capacity at constant pressure, $\text{J}/(\text{kg K})$
c_v	specific heat capacity at constant volume, $\text{J}/(\text{kg K})$
h	enthalpy, J/kg
\dot{m}	mass flow rate, kg/s
M	molecular weight, g/mol
T	temperature, K
T_r	reduced pressure, (T/T_{cr})
P	pressure, bar
PP	pinch point, K
ΔT_{sh}	amount of superheat, K
η	efficiency
η_L	saturated liquid viscosity, Pa s
η_v	saturated vapour viscosity, microPoise
λ_L	saturated liquid thermal conductivity, $\text{W}/(\text{m K})$
λ_v	saturated vapour thermal conductivity, $\text{W}/(\text{m K})$
σ	surface tension, N/m

Subscripts and superscripts

1-4	ORC state points
b	boiling point
c	heat sink
cr	critical point
e	expander
h	heat source
i	inlet
o	outlet
p	pinch point/pump

Acknowledgments

This work was supported by the UK Engineering and Physical Sciences Research Council (EPSRC) [grant number EP/P004709/1]. Data supporting this publication can be obtained on request from cep-lab@imperial.ac.uk.

References

- [1] Markides, C. N., Low-concentration solar-power systems based on organic Rankine cycles for distributed-scale applications: Overview and further developments. *Frontiers in Energy Research*. 2015; 3; 1-16.
- [2] Badr, O., Probert, S. D., O'Callaghan, P. W., Selecting a working fluid for a Rankine-cycle engine. *Applied Energy*. 1985; 21(1); 1-42.
- [3] Chen, H., Goaswami, D. Y., Stefanakos, E. K., A review of thermodynamic cycles and working fluids for the conversion of low-grade heat. *Renewable and Sustainable Energy Reviews*. 2010; 14(9); 3059-3067.
- [4] Saleh, B., Koglbauer, G., Wendland, M., Fischer, J., Working fluids for low-temperature organic Rankine cycles. 2007; 32(7); 1210-1221.
- [5] Tchanche, B. F., Papadakis, G., Lambrinos, G., Frangoudakis, A., Fluid selection for a low-temperature solar organic Rankine cycle. *Applied Thermal Engineering*. 2009; 29(11-12); 2468-2476.
- [6] Papadopoulos, A. I., Strijepovic, M., Linke, P., On the systematic design and selection of optimal working fluids for organic Rankine cycles. *Applied Thermal Engineering*. 2009; 30(6-7); 760-769.
- [7] Palma-Flores, O., Flores-Tlacuahuac, A., Canseco-Melchorb, G., Simultaneous molecular and process design for waste heat recovery. *Energy*. 2016; 99; 32-47.
- [8] Schilling, J., Lampe, M., Gross, J., Bardow, A., 1-stage CoMT-CAD: An approach for integrated design of ORC process and working fluid using PC-SAFT. *Chem. Eng. Sci*. 2016; 153; 217-230.
- [9] Andreasen, J. G., Kærn, M. R., Pierobon, L., Larsen, U., Haglind, F., Multi-objective optimization of organic Rankine cycle power plants using pure and mixed working fluids. *Energies*. 2016; 9; 322.
- [10] Oyewunmi, O. A., Markides, C. N., Thermo-economic and heat transfer optimization of working-fluid mixtures in a low-temperature organic Rankine cycle system. *Energies*. 2016; 9; 448.
- [11] Process Systems Enterprise Ltd, gPROMS v 4.2.0. Available at: <http://www.psenderprise.com> [Accessed 23/11/2016].
- [12] White, M. T., Oyewunmi, O. A., Haslam, A. J., Markides, C. N., High-efficiency industrial waste-heat recovery through computer-aided integrated working-fluid and ORC system optimisation. In: *SusTEM 2017: The 4th Sustainable Thermal Energy Management International Conference*; 2017 Jun 28-30; Alkaar, Netherlands.
- [13] Papaioannou, V., Lafitte, T., Avendaño, C., Adjiman, C. S., Jackson, G., Müller, E. A., Galindo, A., Group contribution methodology based on the statistical associating fluid theory for heteronuclear molecules formed from Mie segments. *J. Chem. Phys.* 2014; 140; 054107.
- [14] Dufal, S., Papaioannou, V., Sadeqzadeh, M., Pogiatis, T., Chremos, A., Adjiman, C. S., Galindo, A., Prediction of thermodynamic properties and phase behaviour of fluids and mixtures with the SAFT- γ Mie group-contribution equation of state. *J. Chem. Eng. Data* 2014; 9(10); 3272-3288.
- [15] Odele, O., Macchietto, S., Computer aided molecular design: A novel method for optimal solvent selection. *Fluid Phase Equilibria* 1993; 82; 47-54.
- [16] White, M. T., Oyewunmi, O. A., Haslam, A. J., Markides, C. N., High-efficiency industrial waste-heat recovery through computer-aided integrated working-fluid and ORC system optimisation. *Energy Conversion and Management*: under review.
- [17] K. G. Joback, R. C. Reid, Estimation of pure-component properties from group-contributions, *Chemical Engineering Communications* 57 (1-6) (1987) 233-243.
- [18] S. Sastri, K. Rao, A new group contribution method for predicting viscosity of organic liquids, *The Chemical Engineering Journal* 50 (1) (1992) 9-25.
- [19] D. Reichenberg, The viscosity of organic vapors at low pressures, *DSC Rep* 11 (1971) 484.
- [20] D. Reichenberg, The estimation of the viscosities of gases and gas mixtures, in: *Symposium on Transport Properties of Fluids and Fluid Mixtures, Their Measurement, Estimation, Correlation and Use*, East Kilbride, Glasgow, Scotland, 1979.

- [21] S. Sastri, K. Rao, Quick estimating for thermal conductivity, *Chemical Engineering* 100 (8) (1993) 106.
- [22] T. H. Chung, L. L. Lee, K. E. Starling, Applications of kinetic gas theories and multiparameter correlation for prediction of dilute gas viscosity and thermal conductivity, *Industrial & Engineering Chemistry Fundamentals* 23 (1) (1984) 8-13.
- [23] T. H. Chung, M. Ajlan, L. L. Lee, K. E. Starling, Generalized multiparameter correlation for nonpolar and polar fluid transport properties, *Industrial & Engineering Chemistry Research* 27 (4) (1988) 671-679.
- [24] S. Sastri, K. Rao, A simple method to predict surface tension of organic liquids, *The Chemical Engineering Journal and the Biochemical Engineering Journal* 59 (2) (1995) 181-186.
- [25] Quoilin S, Declaye S, Tchanche BF, Lemort V. Thermo-economic optimization of waste heat recovery Organic Rankine Cycles. *Appl Therm Eng.* 2011;31(14):2885–93.
- [26] Bergman TL, Lavine AS, Incropera FP, DeWitt DP. *Fundamentals of Heat and Mass Transfer*. John Wiley & Sons; 2011. 1-1048 p.
- [27] Gnielinski V. New Equations for Heat and Mass Transfer in Turbulent Pipe and Channel Flow. *Int Chem Eng.* 1976;(16):359–68.
- [28] Hewitt GF, Shires GL, Bott TR. *Process heat transfer*. CRC Press; 1994.
- [29] Verein Deutscher Ingenieure V. VDA Heat Atlas. In: *VDI Heat Atlas*. Second. Springer; 2010.
- [30] Dobson MK, Wattelet JP, Chato JC. *Optimal Sizing of Two-Phase Heat Exchangers*. 1993.
- [31] Shah M. M., A general correlation for heat transfer during film condensation inside pipes. *Int J Heat Mass Transf.* 1979; 22(4); 547-556.
- [32] Solutia. *Therminol 66: High performance, highly stable heat transfer fluid*. 2016.
- [33] NIST. Reference Fluid Thermodynamic and Transport Properties Database (REFPROP) NIST: National Institute of Standards and Technology; 2016. Available from: <http://www.nist.gov/srd/nist23.cfm>